Role of Extracellular RNA in Atherosclerotic Plaque Formation in Mice

Sakine Simsekyilmaz, Hector A. Cabrera-Fuentes, Svenja Meiler, Sawa Kostin, Yvonne Baumer, Elisa A. Liehn, Christian Weber, William A. Boisvert, Klaus T. Preissner and Alma Zernecke

Circulation. 2014;129:598-606; originally published online November 7, 2013;
doi: 10.1161/CIRCULATIONAHA.113.002562
Circulation is published by the American Heart Association, 7272 Greenville Avenue, Dallas, TX 75231

Print ISSN: 0009-7322. Online ISSN: 1524-4539

Role of Extracellular RNA in Atherosclerotic Plaque Formation in Mice

Sakine Simsekyilmaz, PhD*; Hector A. Cabrera-Fuentes, MSc*; Svenja Meiler, PhD; Sawa Kostin, PhD, MD; Yvonne Baumer, PhD; Elisa A. Liehn, MD, PhD; Christian Weber, MD; William A. Boisvert, PhD; Klaus T. Preissner, PhD†; Alma Zernecke, MD†

Background—Atherosclerosis and vascular remodeling after injury are driven by inflammation and mononuclear cell infiltration. Extracellular RNA (eRNA) has recently been implicated to become enriched at sites of tissue damage and to act as a proinflammatory mediator. Here, we addressed the role of eRNA in high-fat diet–induced atherosclerosis and neointima formation after injury in atherosclerosis-prone mice.

Methods and Results—The presence of eRNA was revealed in atherosclerotic lesions from high-fat diet–fed low-density lipoprotein receptor–deficient ($Ldlr^{-/-}$) mice in a time-progressive fashion. RNase activity in plasma increased within the first 2 weeks (44±9 versus 70±7 mU/mg protein; P=0.0012), followed by a decrease to levels below baseline after 4 weeks of high-fat diet (44±9 versus 12±2 mU/mg protein; P<0.0001). Exposure of bone marrow–derived macrophages to eRNA resulted in a concentration-dependent upregulation of the proinflammatory mediators tumor necrosis factor-α, arginase-2, interleukin-1β, interleukin-6, and interferon-γ. In a model of accelerated atherosclerosis after arterial injury in apolipoprotein E–deficient ($ApoE^{-/-}$) mice, treatment with RNase1 diminished the increased plasma level of eRNA evidenced after injury. Likewise, RNase1 administration reduced neointima formation in comparison with vehicle-treated $ApoE^{-/-}$ controls (25.0±6.2 versus 46.9±6.9×10^3 μm^2, P=0.0339) and was associated with a significant decrease in plaque macrophage content. Functionally, RNase1 treatment impaired monocyte arrest on activated smooth muscle cells under flow conditions in vitro and inhibited leukocyte recruitment to injured carotid arteries in vivo.

Conclusions—Because eRNA is associated with atherosclerotic lesions and contributes to inflammation-dependent plaque progression in atherosclerosis-prone mice, its targeting with RNase1 may serve as a new treatment option against atherosclerosis. **(*Circulation*. 2014;129:598-606.)**

Key Words: atherosclerosis ■ inflammation ■ nucleic acids ■ vascular diseases

Atherosclerosis and its sequelae are the most frequent cause of death in Western societies. The continuing age-related narrowing of (coronary) arteries can necessitate the need for percutaneous transluminal angioplasty. The long-term effects of such therapy, however, are still limited by an excessive arterial remodeling and restenosis.[1,2]

Clinical Perspective on p 606

We have previously shown that extracellular RNA (eRNA) can exert prothrombotic and inflammatory properties in the vasculature. eRNA functions as a cofactor in protease autoactivation of contact-phase coagulation factors[3,4] and of vascular endothelial growth factor– and vascular endothelial growth factor receptor 2–coupled signaling pathways,[5,6] and it may induce cytokine mobilization and liberatio from inflammatory cells.[7] Moreover, systemic treatment with RNase1 was shown to rescue mice from arterial thrombotic occlusion to limit cerebral edema and infarct size after acute stroke, and to serve as a potent anti-inflammatory regimen in vitro and in vivo.[3,5,7–9]

Based on these previous results and the contribution of eRNA to inflammatory processes, we have here investigated the role of eRNA in high-fat diet–induced atherosclerosis in low-density lipoprotein receptor–deficient ($Ldlr^{-/-}$) mice and

Received March 12, 2013; accepted October 28, 2013.

From the Institute for Molecular Cardiovascular Research, RWTH University Hospital Aachen, Aachen, Germany (S.S., E.A.L.); Department of Biochemistry, Medical School, Justus-Liebig-University, Giessen, Germany (H.A.C.-F., K.T.P.); Department of Microbiology, Kazan Federal University, Kazan, Russian Federation (H.A.C.-F.); Center for Cardiovascular Research, John A. Burns School of Medicine, University of Hawaii, Honolulu, HI (S.M., Y.B., W.A.B.); Core Lab for Molecular and Structural Biology, Max-Planck-Institute for Heart and Lung Research, Bad Nauheim, Germany (S.K.); Institute for Cardiovascular Prevention, Ludwig-Maximilians-University, Munich, Germany (C.W.); DZHK (German Centre for Cardiovascular Research), partner site Munich Heart Alliance, Munich, Germany (C.W., A.Z.); Rudolf Virchow Center and Institute of Clinical Biochemistry and Pathobiochemistry, University Hospital Würzburg, University of Würzburg, Würzburg, Germany (A.Z.); and Department of Vascular Surgery, Klinikum rechts der Isar, Technical University, Munich, Germany (A.Z.).

*Dr Simsekyilmaz and Cabrera-Fuentes contributed equally to this work as first authors.

†Drs Preissner and Zernecke contributed equally to this work as senior authors.

The online-only Data Supplement is available with this article at http://circ.ahajournals.org/lookup/suppl/doi:10.1161/CIRCULATIONAHA.113.002562/-/DC1.

Correspondence to Alma Zernecke, MD, Institute of Clinical Biochemistry and Pathobiochemistry, University of Würzburg, Josef-Schneider-Str. 2, D-97080 Würzburg, Germany. E-mail alma.zernecke@uni-wuerzburg.de

in a model of accelerated plaque formation in carotid arteries after injury in apolipoprotein E–deficient (*ApoE*$^{-/-}$) mice.

Our new data provide strong evidence that eRNA-mediated reactions contribute to inflammation-driven processes in experimental atherosclerosis and vascular remodeling and that administration of RNase1 serves as a new intervention modality for protection from atherogenesis.

Methods

Mouse Models of Atherosclerosis and Intravital Microscopy

Wild-type and *Ldlr*$^{-/-}$mice (both on the C57BL/6J background, n=6 per group) were obtained from the Jackson Laboratory (Bar Harbor, ME), and *ApoE*$^{-/-}$ mice (C57BL/6J background, n=13–14 per group) from Charles River, Italy. *Ldlr*$^{-/-}$ mice were fed an atherogenic diet as described.[10] *ApoE*$^{-/-}$ mice, placed on an atherogenic high-fat diet (HFD; 21% fat, 0.15% cholesterol) for 1 week before and up to 3 weeks after injury, were anesthetized (100 mg/kg ketamine hydrochloride/10 mg/kg xylazine IP) and subjected to wire-induced arterial injury of the common carotid artery, as described.[11,12] Animals were treated intravenously with a bolus of 0.76 μg of RNase1 (in phosphate-buffered saline) or phosphate-buffered saline alone immediately before arterial injury, and they were continuously treated with RNase1 via Alzet osmotic minipumps (42 μg/kg mouse per day), subcutaneously implanted 1 day before injury. Intravital microscopy was performed 1 day after injury as described.[11] All animal studies were approved by local authorities and complied with German animal protection laws.

Immunohistochemistry and Quantification of RNA

Five-micrometer-thick cryosections of aortic sinus from *Ldlr*$^{-/-}$ mice were used for RNA localization by staining with SYTO RNASelect dye (Invitrogen)[3] and visualizing with confocal microscopy (Nikon Eclipse TE2000-E, Nikon, Japan). Carotid arteries of *ApoE*$^{-/-}$ mice were excised and embedded in paraffin. Neointimal and medial areas were quantified in serial sections within 500 μm from the bifurcation by modified Movat pentachrome staining and planimetry. Adjacent sections were used to assess cellular plaque content by immunofluorescence staining of Mac2^{+} macrophages and α-smooth muscle actin–positive smooth muscle cells (SMCs).[12] For quantification of RNA, sections stained for SMCs with tetramethylrhodamine isothiocyanate–labeled antibody against smooth muscle α-actin, SYTO RNASelect dye and 4′,6-diamidino-2-phenylindole were examined by laser-scanning confocal microscopy (Leica TCS SP2). Each independent experiment represents the mean value of 10 randomly chosen fields of vision in each section, quantified by using 3-dimensional Quantification and VoxelShop options of Imaris 6.3.1 (Bitplane). The area of specific labeling for eRNA was separately calculated as arbitrary fluorescent units of positive labeling per medial area or neointimal area, as previously described.[13]

RNase Activity

At indicated time points, blood was taken from mice for analysis of RNase1 activity by an enzymatic assay, as described.[8] All activity values were normalized to the same protein concentration in different samples.

Isolation of eRNA and Real-Time Polymerase Chain Reaction Analysis

DNA-free total RNA was extracted from serum of mice or cultured cell supernatants by the use of the Zymo RNA MicroPrep kit (Zymo Research), including an additional DNA-digestion step. For real-time polymerase chain reaction analysis, RNA was reverse-transcribed into cDNA at 37°C for 1 hour (BioAnalyzer), and cDNA fragments were amplified by using specific primer pairs (see the online-only Data Supplement for details).

Cell Culture and Cell Adhesion Assay Under Flow

Bone marrow–derived macrophages (BMDMs) were generated from bone marrow cells in macrophage colony-stimulating factor (CSF)–containing L929-conditioned medium as described,[10,14] or by incubation with mouse recombinant macrophage CSF or granulocyte macrophage CSF (50 ng/mL each).[15] Experiments were conducted for 24 hours in 6-well trays (1.5×10^6 cells/mL; Costar, Cambridge, MA) in the absence or presence of eRNA (1, 10, or 25 μg/mL), as indicated. Control cells were treated with growth medium alone (vehicle). For quantitation of tumor necrosis factor-α (TNF-α) and interleukin (IL)-6 protein production, BMDMs were treated with eRNA (1, 10, or 25 μg/mL) for 24 hours, followed by centrifugation and concentration of cell supernatants by using Centricon tubes (Millipore, Frankfurt, Germany) with a cutoff at 10 kDa. TNF-α and IL-6 enzyme-linked immunosorbent assays were performed by using commercially available kits from eBioscience (Frankfurt, Germany). Total protein concentration was determined with the use of the BCA kit from Thermo-Fisher Scientific (Bonn, Germany). Human coronary artery SMCs (Promocell) and MonoMac6 cells were maintained, as described.[11,16] MonoMac6 cell adhesion to SMCs was analyzed in parallel-wall flow chambers.[11] Confluent SMCs were activated with eRNA (1, 10, or 25 μg/mL), or TNF-α (50 ng/mL) in the absence or presence of RNase1 (10 μg/mL) for 16 hours.

Viability Assay

Viability assays were performed after treating SMCs and MonoMac6 cells with RNase1 (10 μg/mL) for 30 minutes or 16 hours by the use of the fluorescent CellTiter-Blue cell viability assay (Promega, Mannheim, Germany).

Statistics

Data were analyzed by unpaired Student *t* tests or 1-way analysis of variance followed by Tukey or Dunnett multiple-comparison post tests (detailed in the online-only Data Supplement). Differences with $P<0.05$ were considered to be statistically significant.

Results

eRNA Accumulates Within Lesions Whereas Plasma RNase Activity Decreases With the Progression of Atherosclerosis

The presence of eRNA was evaluated by immunohistochemical staining in aortic root tissue from 8-week-old *Ldlr*$^{-/-}$ mice fed a chow diet and *Ldlr*$^{-/-}$ mice fed a HFD for 8, 12, or 36 weeks in comparison with chow-fed Bl6 wild-type mice. Although no eRNA was detected in chow-fed Bl6 or *Ldlr*$^{-/-}$ mice (RNA staining detectable in 4′,6-diamidino-2-phenylindole–positive cell nuclei only), eRNA accumulated in atherosclerotic lesions of HFD-fed *Ldlr*$^{-/-}$ mice in a time-progressive fashion (Figure 1). Quantification of eRNA showed a continuous increase in both the media and intima of *Ldlr*$^{-/-}$ mice with increasing durations of HFD feeding, whereas relative staining for eRNA increased in the media, exceeding that in the intima at early time points; eRNA was abundantly present predominantly in the intima at later time points, as reflected by an intense staining in this area (Figures 1 and 2A). After 36 weeks of HFD, eRNA was detectable not only along the luminal lining and in the vicinity of lesional MOMA-2^{+} macrophages (Figures 1E and 2B through 2E), but also within acellular necrotic core areas (Figures 1E and 2F through 2K).

We further assessed RNA-degrading RNase activity in plasma samples from these mice during the course of HFD

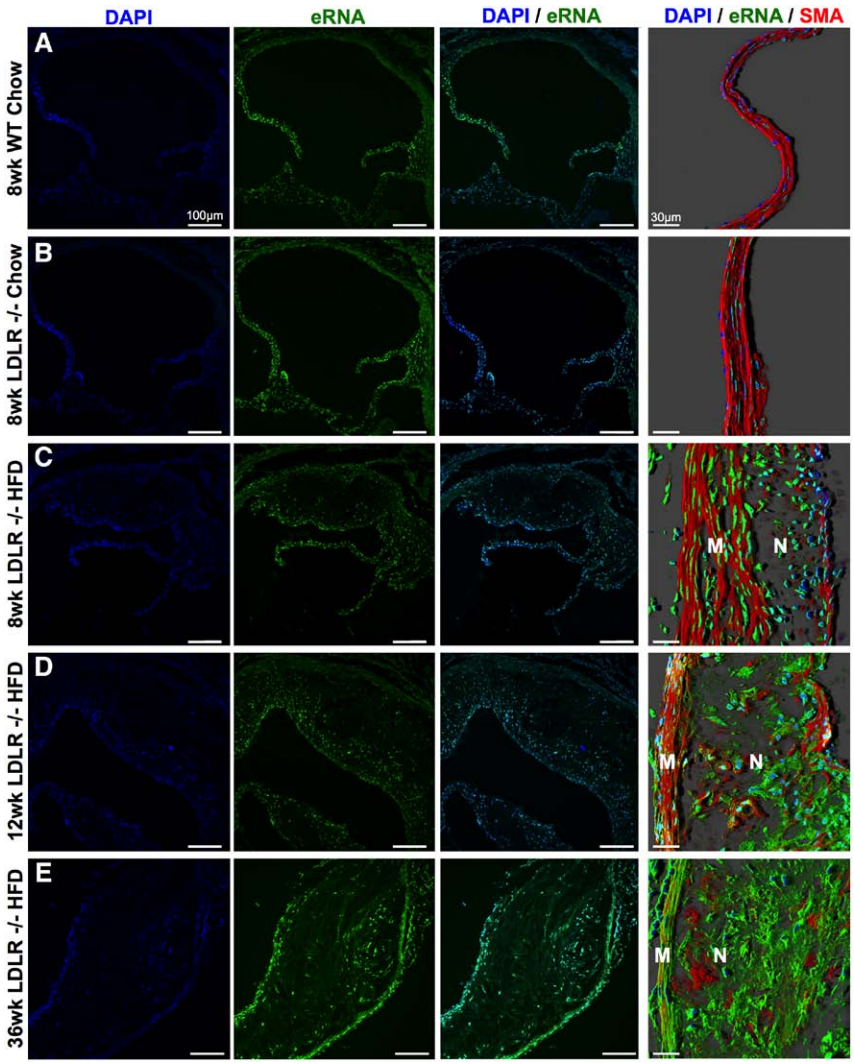

Figure 1. Time-progressive distribution of extracellular RNA (eRNA) in atherosclerotic lesions. The presence of eRNA in aortic root tissue from WT or *Ldlr*$^{-/-}$ mice fed a chow diet for 8 weeks or from *Ldlr*$^{-/-}$ mice fed a high-fat diet (HFD) for 8 (**A** through **C**), 12 (**D**), or 36 weeks (**E**), as indicated, was demonstrated by confocal microscopy with the use of an RNA-binding fluorescence dye (RNA Select, green) together with cell nuclei staining (4′,6-diamidino-2-phenylindole [DAPI], blue). The right-hand panels in each line are confocal images with merged immunostaining for eRNA (green), cell nuclei (DAPI, blue), and smooth muscle actin (SMA, red). M indicates media; and N, neointima (n=6 per group).

feeding, and we observed a biphasic characteristic with a temporary increase during the first 2 weeks (44±9 versus 70±7 mU/mg protein; P=0.0012), followed by a significant and sustained decrease to ≈20% to 40% of the activity in baseline controls, starting at 4 weeks of HFD feeding (44±9 versus 12±2 mU/mg protein; P<0.0001; Figure 2L).

These data indicate that plasma RNase activity is enhanced in early atherosclerosis, but decreases during further plaque growth, when eRNA accumulates within atherosclerotic lesions in a time-progressive manner.

eRNA Enhances Cytokine Secretion From Macrophages

Given the association of eRNA with macrophages within atherosclerotic lesions, we assessed whether eRNA induces inflammatory responses in macrophages. On 24 hours of stimulation of BMDMs with eRNA in vitro, mRNA expression of proinflammatory cytokines *Tnf-α*, *Arg2*, *Il-1β*, *Il-6*, *Ifn-γ* was significantly upregulated in a concentration-dependent manner, whereas a reciprocal downregulation of the anti-inflammatory cytokines *Il-10* and *Il-4* was observed (Figure 3A). Similarly, recombinant mouse macrophage CSF–driven BMDM differentiation was skewed toward the M1-phenotype by exposure to eRNA, resulting in the overexpression of inflammatory markers such as *Tnf-α*, *Arg2*, *Il-1β*, *Il-6*, and *Ifn-γ* together with *Il-12* and inducible nitric oxide synthase (*iNOS*), whereas anti-inflammatory genes together with *Arg1* and macrophage mannose receptor-2 (*Cd206*) were significantly downregulated by eRNA (Figure 3B). The capacity of granulocyte macrophage CSF–driven BMDM differentiation (already representing an M1-phenotype)[15,17] toward further M1 polarization in response to eRNA was moderate; nevertheless, a significant downregulation of M2 markers was confirmed (Figure I in the online-only Data Supplement). In accordance with our proposal, these data clearly corroborate that self-eRNA serves as an proinflammatory alarming signal.

Accordingly, the release of TNF-α and IL-6 proteins into the cell supernatants was significantly increased by eRNA stimulation in a concentration-dependent manner (Figure 3C and 3D). We furthermore assessed whether these effects were mediated by eRNA-induced Toll-like receptor (TLR)–mediated signaling. Based on findings that no changes in *Stat1* expression were found in macrophages on stimulation with eRNA (Figure 3A and 3B, and Figure I in the online-only Data Supplement), we can conclude that eRNA does not

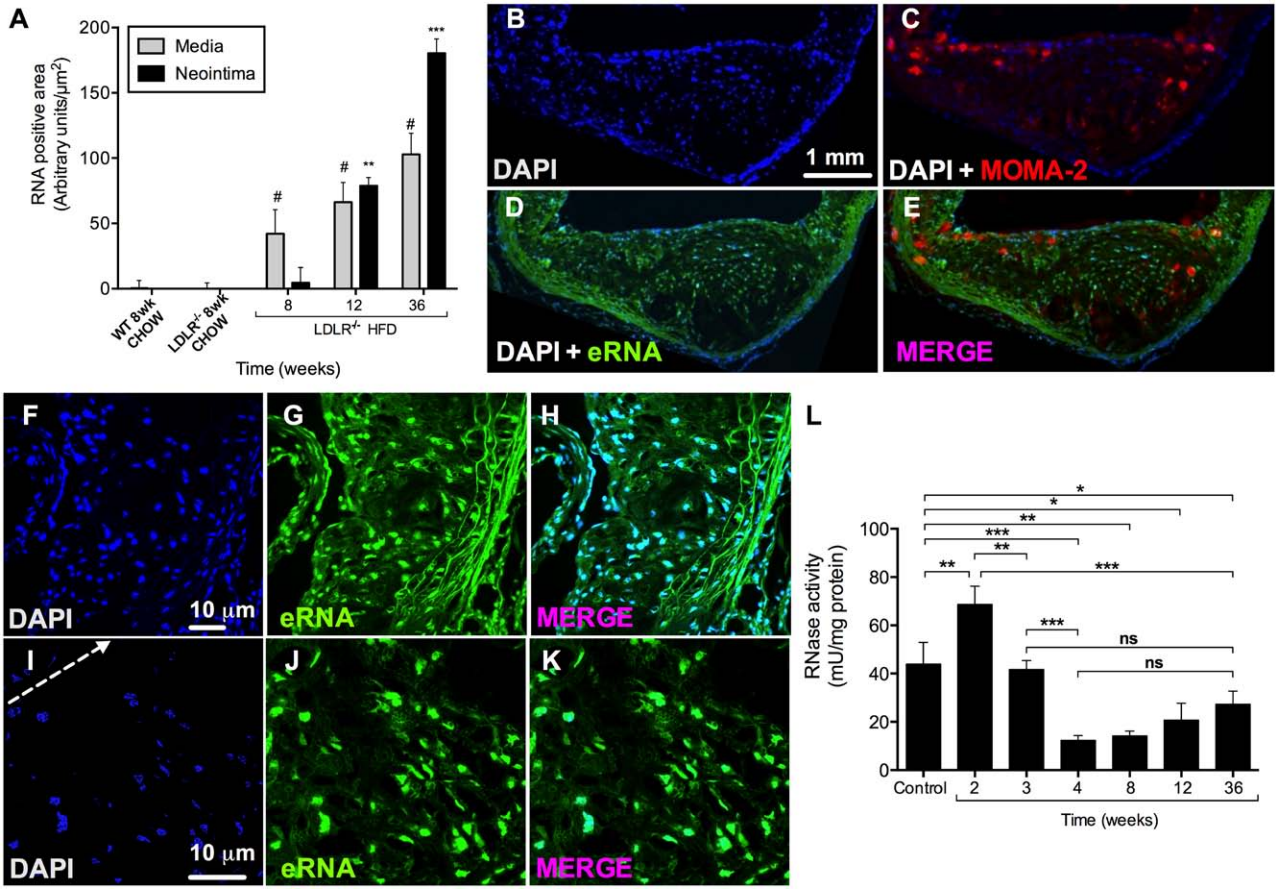

Figure 2. Colocalization of eRNA and macrophages in atherosclerotic lesions of *Ldlr*$^{-/-}$ mice after 36 weeks on HFD, and RNase activity in mouse plasma. **A,** Quantitative analysis of eRNA-associated fluorescence intensity in aortic root tissue in the media and neointima in wild-type (WT) and *Ldlr*$^{-/-}$ mice fed a normal chow or HFD for indicated time periods. Values are expressed as mean±SD (n=6 per group); #*P*<0.05 vs media, and ***P*<0.001 vs neointima in chow-fed *Ldlr*$^{-/-}$ mice. **B** through **E**, Immunofluorescence staining in cryosections of atherosclerotic lesions from *Ldlr*$^{-/-}$ mice after 36 weeks on HFD. Staining for eRNA (**D**) was performed by an RNA-binding fluorescence dye (RNA Select, green), macrophages (**C**) were identified by the anti-MOMA-2 monoclonal antibody (red), and cell nuclei (**B**) were marked by DAPI staining (blue). **E** through **K**, Higher magnifications of atherosclerotic lesions are shown stained with DAPI (blue, **F** and **I**; arrow indicates cellular toward acellular necrotic core regions) and RNA-binding fluorescence dye (green, **G** and **J**); merged images are indicated in **H** and **K**. All images were obtained under identical conditions of confocal laser beam intensity and exposure time; representative images are displayed (n=4). **L**, RNase activity in *Ldlr*$^{-/-}$ mouse plasma was quantified for each time point and normalized to plasma protein concentration. Values are expressed as mean±SD (n=6–12 per group); **P*<0.05, ***P*<0.01, ****P*<0.001. DAPI indicates 4′,6-diamidino-2-phenylindole; eRNA, extracellular RNA; HFD, high-fat diet; MOMA-2, anti-monocyte + macrophage antibody; ns, nonsignificant; and SD, standard deviation.

engage in TLR-2 and TLR-4 signaling.[18] Likewise, no alterations in the mRNA expression of the cytokines studied were observed after poly(IC) treatment (data not shown), indicating that also TLR-3 did not contribute to eRNA-mediated cytokine induction. Thus, eRNA functions as a powerful inducer of inflammatory cytokine responses in macrophages, independent of TLR-2, TLR-3, and TLR-4 signaling.

eRNA Serves as Damage Marker in Experimental Atherosclerosis

To assess the functional role of eRNA in lesion growth, a model of injury-induced, accelerated atherosclerosis was used. After injury, apolipoprotein E-deficient (*ApoE*$^{-/-}$) mice displayed a marked increase in eRNA at 1 day and 1 week after injury (Figure 4A).

eRNA may be released from activated, damaged, or necrotic cells during injury and is composed mainly of ribosomal RNA (≈85%), transfer RNA (≈10%), and mRNA (≈5%).[4,8] We therefore determined the source of eRNA by analyzing the expression of specific mRNA species, indicative of the originating cell type. Quantitative polymerase chain reaction analysis revealed that both *Cd31* mRNA, used as a marker for endothelial cells, and *αSMA* mRNA as a marker for SMCs, as well, were increased in plasma at day 1 but not immediately after injury (Figure 4B). These data indicate that endothelial cells and SMCs release eRNA into the extracellular space during and after arterial injury.

Notably, eRNA was increased in supernatants of SMCs in a time-dependent manner when cells were treated with TNF-α (Figure 4C), indicating that SMCs may release eRNA also during cell activation.

Treatment of *ApoE*$^{-/-}$ Mice With RNase1 Diminishes Experimental Atherosclerosis

To investigate if eRNA directly or indirectly contributes to neointima formation after arterial injury, *ApoE*$^{-/-}$ mice fed a

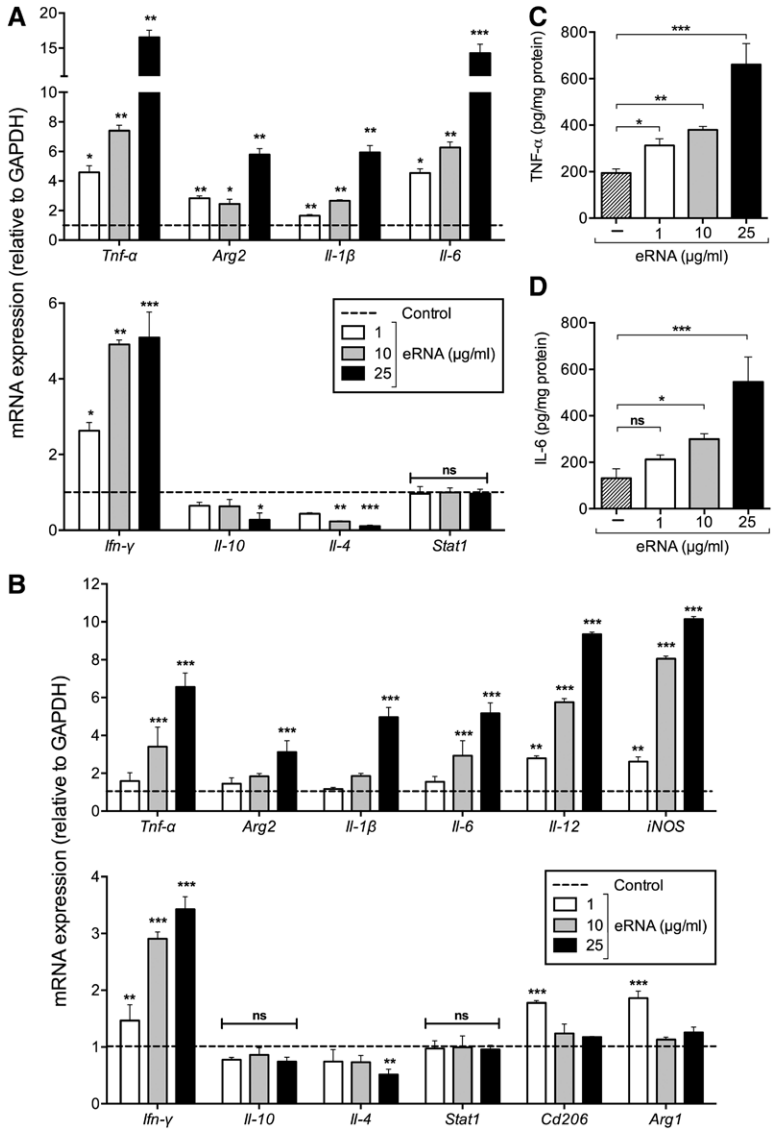

Figure 3. Influence of eRNA on pro- and anti-inflammatory mediators in bone marrow–derived macrophages (BMDMs). **A**, mRNA expression of *Tnf-α, Arg2, Il-1β, Il-6*, *Ifn-γ, Il-10*, *Il-4*, and *Stat1* in wild-type BMDMs, differentiated in the presence of M-CSF–containing L929-conditioned medium was analyzed by real-time PCR in the absence (control, dotted line) or presence of eRNA (1, 10, or 25 μg/mL) for 24 hours. Data are expressed as changes in the ratio between target gene expression and *Gapdh* mRNA. Values represent mean±SD (n=6 per group); **P*<0.05, ***P*<0.01, ****P*<0.001 vs control. **B,** mRNA expression of *Tnf-α, Arg2, Il-1β, Il-6*, *Il-12, iNOS, Ifn-γ, Il-10*, *Il-4*, *Stat1, Cd206*, and *Arg1* in wild-type BMDMs, differentiated in the presence of mouse recombinant M-CSF, was analyzed by real-time PCR in the absence (control, dotted line) or presence of eRNA (1, 10, or 25 μg/mL) for 24 hours. Data are expressed as changes in the ratio between target gene expression and *Gapdh* mRNA. Values represent mean±SD (n=6 per group); **P*<0.05, ***P*<0.01, ****P*<0.001 vs control. TNF-α (**C**) or IL-6 (**D**) protein concentration was measured in the supernatants of BMDM after treatment in the absence (control) or presence of eRNA (1, 10, or 25 μg/mL) as indicated. Values correspond to mean±SD (n=9 per group). **P*<0.05, ***P*<0.01, ****P*<0.001. eRNA indicates extracellular RNA; IL-6, interleukin 6; M-CSF, macrophage colony-stimulating factor; ns, nonsignificant; PCR, polymerase chain reaction; SD, standard deviation; and TNF-α, tumor necrosis factor-α.

HFD and treated with RNase1 or vehicle (phosphate-buffered saline) alone were subjected to wire-induced injury of the common carotid artery. RNase activity was markedly elevated in RNase1-treated mice, but not in control mice, throughout the 3-week study period (Figure II in the online-only Data Supplement). Moreover, RNase1 treatment inhibited the increase in eRNA (Figure 4A), and similarly diminished *Cd31* and *αSMA* mRNA appearance in plasma after injury in comparison with control-treated *ApoE*$^{-/-}$ mice (Figure 4B), confirming the efficiency of the treatment.

Neointima formation was assessed at 1 and 3 weeks after injury and revealed a trend toward reduced neointima formation at 1 week after injury and a significant reduction by 47% after 3 weeks in RNase1-treated mice in comparison with controls (25.0±6.0×10^3 μm^2, n=8 mice, versus 46.9±6.8×10^3 μm^2, n=7 mice, *P*=0.0136), whereas medial areas were diminished at 1 week (32.0±1.3 versus 53.2±5.1×10^3 μm^2, n=3 mice each, *P*=0.0159) but remained unaltered at 3 weeks after injury (Figure 5A). This was accompanied by a reduction in relative Mac-2$^+$ macrophage plaque content (17.1±4.4% versus 61.2±7.6%, *P*<0.0001) but an increase of α-smooth muscle actin–positive SMC area at 3 weeks after injury (22.6±1.9 versus 15.4±4.2%, *P*=0.0339) (Figure 5B and 5C), suggesting a reduction in mononuclear cell infiltration and a more stable plaque phenotype in RNase1-treated mice.

Importantly, a significant upregulation of *Tnf-α* transcripts were observed at 1 day, 1 week, and 3 weeks and of *Il-1β* and *Il-6* at 1 day after injury in comparison with carotid arteries before injury, which was significantly reduced by RNase1 treatment (Figure 6A through 6C). Moreover, the injury-induced sustained induction of the adhesion molecules *Vcam-1*, *Icam-1*, *P-selectin*, and *Ccl2* was abrogated in RNase1-treated mice (Figure 6D through 6G). In line, immunofluorescence staining of TNF-α and intercellular adhesion molecule 1 protein in the arterial vessel wall, performed at 1 week after injury, was reduced in RNase1-treated mice (Figure 6H and 6I). These data demonstrate that the retardation in plaque growth induced by RNase1 treatment was associated with a diminished expression of inflammatory cytokines and adhesion molecules in inflamed arteries in vivo.

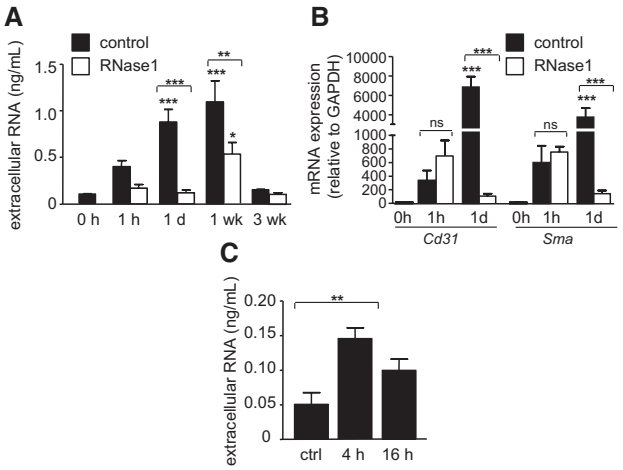

Figure 4. eRNA increases after vascular injury. **A,** The concentration of eRNA in plasma of *ApoE*$^{-/-}$mice before injury (0 hours) and at indicated time points after arterial injury was measured in the control (filled bars) and the RNase1 treatment group (open bars). Values are expressed as mean±SEM (n=7 per group). **P*<0.05, ***P*<0.01, ****P*<0.001 vs 0 hour control, or as indicated. **B,** mRNA detection for *Cd31* (endothelial cells) and α-smooth muscle actin (*Sma*, smooth muscle cells) in plasma before injury (0 hours), at 1 hour and 1 day after injury (n=4–5 per group) was quantified by real-time PCR in the control (filled bars) and RNase1 treatment group (open bars). Values are expressed as mean±SEM; **P*<0.05, ***P*<0.01, ****P*<0.001 vs 0 hour, or as indicated; **C,** eRNA concentration was measured in supernatants of SMC activated with TNF-α for 4 or 16 hours. Values represent mean±SEM (n=6 per group); **P*<0.05. eRNA indicates extracellular RNA; ns, nonsignificant; PCR, polymerase chain reaction; and SEM, standard error of the mean.

eRNA Mediates Monocyte Recruitment In Vitro and in Experimental Atherosclerosis

It was previously shown that eRNA promotes leukocyte adhesion in the vasculature of the cremaster muscle and induces the expression of intercellular adhesion molecule-1 in endothelial cells in vitro.[7] Similarly, treatment of SMCs with eRNA induced a mild but significant and concentration-dependent upregulation of the expression of *Vcam-1*, *Icam-1*, *P-selectin*, and *Ccl2* with a maximal response at 10 μg/mL (Figure III in the online-only Data Supplement). To test whether eRNA may also facilitate monocyte recruitment to SMCs, we monitored monocytic MonoMac6 cell adhesion to TNF-α–activated SMCs. Although MonoMac6 cells did not adhere to unstimulated SMCs (not shown), MonoMac6 cell adhesion supported by activated SMCs was significantly reduced when SMCs were pretreated with RNase1; pretreatment of MonoMac6 cells did not affect cell adhesion per se (Figure 7A). Treatment with RNase1 did not consistently alter the expression of adhesion molecules *Icam-1*, *Vcam-1*, *P-selectin,* or *Ccl2* in untreated or TNF-α–activated SMCs (not shown). Moreover, RNase1 pretreatment of untreated or TNF-α–stimulated MonoMac6 cells or SMCs did not reduce cell viability (not shown). Thus, these collected data were not attributable to any direct changes in adhesion molecules in SMCs or a cytotoxic effect of RNase1.

We further assessed whether eRNA may also contribute to leukocyte recruitment to injured arteries in vivo. To this end, intravital microscopy was performed 1 day after injury in carotid arteries of *ApoE*$^{-/-}$ mice, treated with vehicle (phosphate-buffered saline) only in comparison with RNase1 administration. Notably, leukocyte adhesion to injured artery segments was substantially reduced in RNase1-treated *ApoE*$^{-/-}$ mice in comparison with vehicle-treated mice (14.6±1.7 cells/HPF, n=6 mice, versus 8.2±2.3 cells/high power field, n=7 mice, *P*=0.0491; Figure 7B). These findings indicate that eRNA accumulation following injury may directly or indirectly (eg, via TNF-α) contribute to leukocyte recruitment and plaque formation in vivo.

Discussion

In the present study, the multifunctional eRNA/RNase system was characterized for its contribution to chronic vascular disease as it relates to the progression of atherosclerotic lesion formation in two established mouse models. Our data indicate that (1) in *Ldlr*$^{-/-}$ mice fed a HFD, eRNA accumulates in atherosclerotic plaques in a time-dependent manner, can be released from activated cells, and is increased in plasma of *ApoE*$^{-/-}$ mice after arterial injury; (2) conversely, a biphasic characteristic for plasma RNase activity was observed with an increase soon after the initiation of HFD, and a decline to levels below baseline during progressive plaque growth;

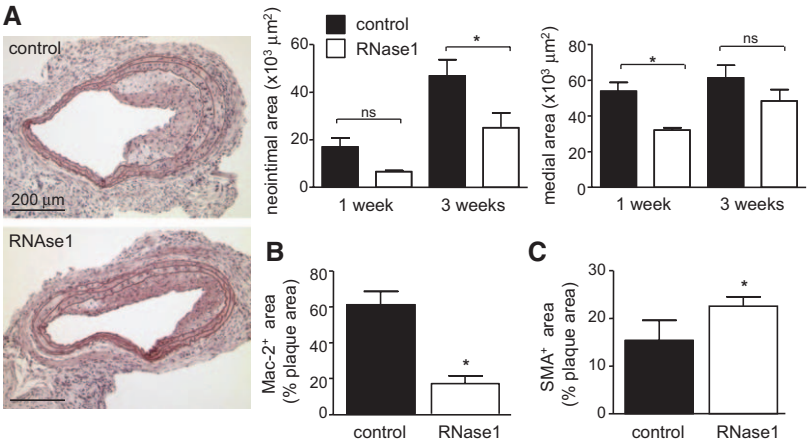

Figure 5. RNase1 treatment of atherosclerosis-prone *ApoE*$^{-/-}$ mice protects from neointimal plaque formation. **A** through **C,** *ApoE*$^{-/-}$ mice fed a high-fat diet and treated vehicle (PBS, filled bars) or RNase1 (open bars) were subjected to wire-induced injury of the common carotid artery. Neointimal and medial areas were assessed 1 week (n=3 per group) and 3 weeks (n=7–8 per group) after injury. Values represent mean±SEM; **P*<0.05. **A,** Representative images of pentachrome-stained sections at 3 weeks after injury are documented. Quantification of the relative content of Mac-2–positive neointimal macrophages (**B**) and α-SMA–positive SMCs (**C**), as well, are indicated in the control group (filled bars) in comparison with the RNase1 treatment group (open bars) 3 weeks after injury. Values represent mean±SEM; **P*<0.05. ns indicates nonsignificant; PBS, phosphate-buffered saline; SEM, standard error of the mean; α-SMA, α-smooth muscle actin; and SMC, smooth muscle cell.

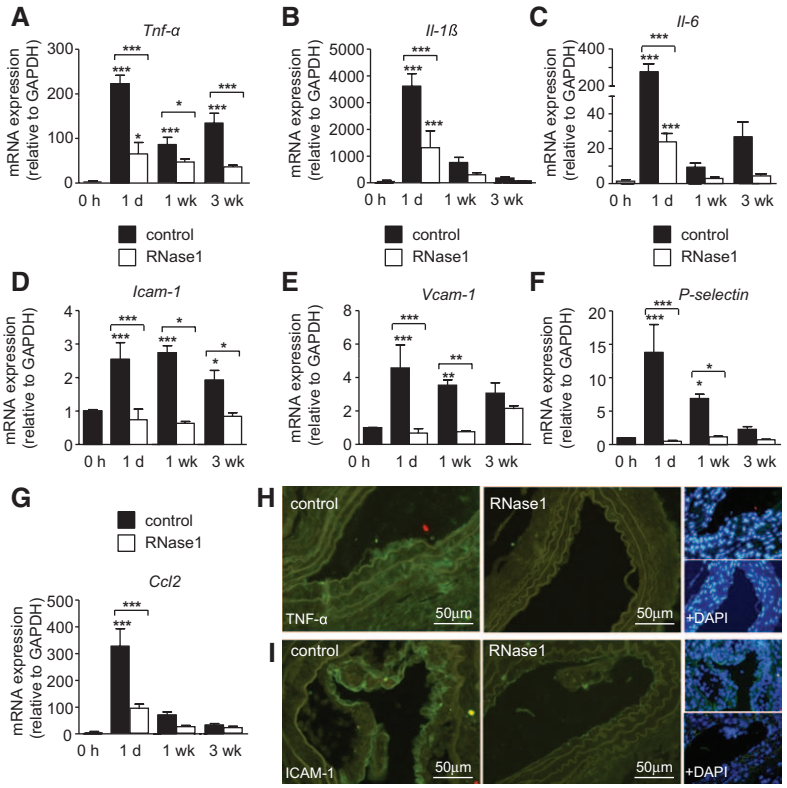

Figure 6. RNase1 treatment of atherosclerosis-prone *ApoE*$^{-/-}$ mice reduces vascular cytokine and adhesion molecule expression. **A** through **I,** *ApoE*$^{-/-}$ mice fed a high-fat diet and treated with vehicle (PBS, filled bars) or RNase1 (open bars) were subjected to wire-induced injury of the common carotid artery. *Tnf-α* (**A**), *Il-1β* (**B**), *Il-6* (**C**), *Icam-1* (**D**), *Vcam-1* (**E**), *P-selectin* (**F**), and *Ccl2* (**G**) mRNA expression were assessed at indicated time points after injury. Data are expressed as changes in the ratio between target gene expression and *Gapdh* mRNA. Values represent mean±SEM (n=12 per group); **P*<0.05, ***P*<0.01, and ****P*<0.001 versus 0 hours, or as indicated. **H** and **I**, Representative fluorescence images of TNF-α (**H**) and ICAM-1 (**I**) protein expression (green) at 1 week after injury, and together with cell nuclei staining (DAPI, blue). DAPI indicates 4′,6-diamidino-2-phenylindole; ICAM-1, intercellular adhesion molecule 1; PBS, phosphate-buffered saline; SEM, standard error of the mean; and TNF-α, tumor necrosis factor-α.

(3) eRNA induces an inflammatory gene expression in bone-marrow–derived macrophages and increases adhesion molecular expression in SMC; and (4) promotes monocyte adhesion to activated SMC in vitro and to the carotid vessel wall in vivo; (5) RNase1 administration in HFD-fed *ApoE*$^{-/-}$ mice results in significantly reduced neointimal plaque formation, monocyte recruitment, and vascular inflammation after injury. Together, these data provide strong evidence for a major role of the eRNA/RNase system in atherogenesis and establish RNase1 treatment as a potential novel therapeutic regimen.

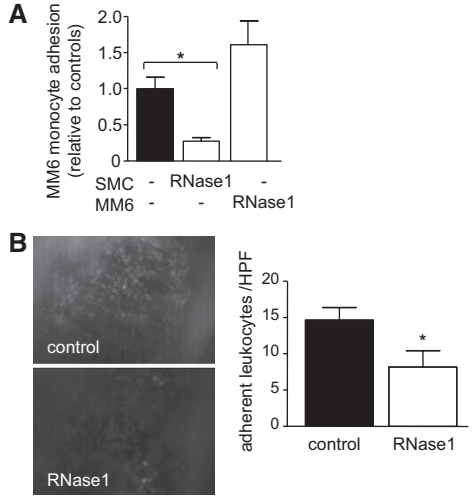

Figure 7. eRNA contributes to monocyte adhesion to activated SMCs and carotid arteries after injury. **A,** MonoMac6 cell adhesion to TNF-α–activated SMCs was analyzed under flow conditions in vitro in the absence (filled bar) or the presence of RNase1 (open bars), as indicated. Values represent mean±SEM (n=6–8 per group). **P*<0.05. **B,** Leukocyte adhesion to carotid arteries of *ApoE*$^{-/-}$ mice treated with vehicle (control) or RNase1 1 day after injury in vivo (n=6–7 per group) was determined. Representative images of rhodamine 6G–labeled leukocytes adhering to carotid arteries (original magnification ×20) and quantitation of results, as well, are shown. Values represent mean±SEM; **P*<0.05. eRNA indicates extracellular RNA; HPF, high power field; SEM, standard error of the mean; SMC, smooth muscle cell; and TNF-α, tumor necrosis factor-α.

Here, we demonstrate for the first time that eRNA accumulates within arterial lesions in the media and at later stages predominantly in the neointima in a time-dependent fashion, as documented by staining of affected vascular sites with an RNA-binding dye in HFD-fed mice, but not in controls. Furthermore, we evidenced an increased eRNA content in plasma after arterial injury in vivo. This may be attributable to the direct release of RNA from damaged tissues, because mRNA (as a portion of eRNA) originating from endothelial cells and SMCs was elevated as well. The TNF-α–induced increase in eRNA released from cultured SMCs furthermore implied that RNA may also be released from cells in the context of inflammation and cytokine exposure after injury. Conversely, we recently demonstrated that eRNA may increase the extracellular concentration of TNF-α by promoting the liberation of transmembrane pro-TNF via the sheddase TNF-α–converting enzyme,[7] such that both reactions may amplify the concentration of TNF-α and other cytokines.

Although eRNA may be degraded by plasma RNases, increased levels of eRNA were similarly detected in patients with tumors, sepsis, or lung fibrosis.[4,8] This led us to propose that eRNA, released under pathological conditions, may become protected against degradation by binding to proteins and phospholipids,[19] or is associated with microparticles or exosomes.[20] However, the biphasic change of vascular

RNases, showing an increase early after the initiation of a HFD diet, but a decrease in the course of chronic lesion formation (observed from 4 weeks on), strongly implies a causal relationship between a dysbalance in the eRNA/RNase system and the initiation and progression of atherosclerosis. No significant changes in RNase activity were noted between wild-type, *Ldlr*$^{-/-}$ and *ApoE*$^{-/-}$ mice (not shown). However, no regulation in RNase activity was noted in *ApoE*$^{-/-}$ mice in the accelerated model of injury-induced atherosclerosis, suggesting that injury-associated factors, such as a massive release of RNA from damaged cells, may have either consumed the atherosclerosis-induced early increase in RNase activity or abrogated its induction.

In accordance with the damaging nature of eRNA, several proinflammatory cytokines (including TNF-α, IL-1β, IL-6) were upregulated in macrophages, whereas a decrease in anti-inflammatory cytokines was demonstrated. This is in line with a shift in macrophage polarization toward the M1-phenotype, and a repression of typical M-2 phenotype markers such as Arg1 or CD206, as well. No involvement of TLRs in self-eRNA–cell interactions was noted. Importantly, the indicated inflammatory cytokines were also increased in carotid arteries after injury in vivo, whereas RNase1 treatment significantly reduced their expression levels in comparison with controls. In essence, the appearance of eRNA in the diseased tissue may thus be considered as an alarm signal that amplifies tissue inflammation by the induction of cytokine production, and the promotion of M1-macrophage polarization and by the release of bioactive TNF-α, as well, as documented earlier,[7] being a potent proatherogenic factor.[16] The latter process may involve direct or indirect activation of TNF-α–converting enzyme by eRNA, as previously demonstrated by our group.[21]

Recently, it was revealed that eRNA not only promotes the adhesion and transmigration of leukocytes in the murine cremaster muscle vasculature, but that it also induces the expression of intercellular adhesion molecule 1 in endothelial cells in vitro.[7] Similarly, we here observed an increase in adhesion molecules intercellular adhesion molecule 1, vascular cell adhesion molecule 1, P-selectin, and CCL2 in SMC, which may likewise contribute to monocyte adhesion to activated SMCs and to leukocyte recruitment in carotid arteries after injury, as well.[22] Importantly, and in line with the proinflammatory function of eRNA, our findings show that the systemic treatment with RNase1 reduced adhesion molecule expression, inhibited leukocyte adhesion, and reduced arterial macrophage accumulation and neointimal plaque formation after injury in carotid arteries of *ApoE*$^{-/-}$ mice in vivo.

eRNA was also demonstrated to mediate vascular permeability via the mobilization/stabilization and direct binding to vascular endothelial growth factor.[5] Enhanced vascular endothelial growth factor signaling induced by eRNA may, in addition, promote monocyte adhesion and plaque expansion.[23]

In addition, eRNA was shown to act as a prothrombotic cofactor. Accordingly, systemic treatment with RNase1 rescued mice from thrombotic occlusion of the carotid artery in a model of arterial thrombosis[3] and reduced cerebral edema and infarction size in acute stroke.[9] Neointimal hyperplasia after arterial injury is characterized by endothelial denudation, exposure of extracellular matrix, and adhesion of activated platelets, which all contribute to inflammatory leukocyte recruitment and neointima formation after injury.[24] By contributing to platelet accumulation at the site of injury, eRNA may thus, in addition, promote injury-induced leukocyte adhesion and neointimal hyperplasia.

The underlying pathogenetic mechanisms of eRNA as a proinflammatory mediator may thus involve both direct and indirect signaling pathways. Our findings thus indicate that eRNA serves as an important inflammatory mediator after vascular injury, identifying extracellular ribonucleic acids as a new target for the treatment of inflammation during vascular remodeling.

The present study provides novel experimental evidence for the multifunctional properties of self-eRNA as an important trigger of different inflammatory processes that fuel atherogenesis and may culminate in atherosclerotic lesion growth. Our experimental data show that administration of RNase1 abrogates the detrimental functions of eRNA, and provide promising evidence for the establishment of novel interventional strategies for the therapy of cardiovascular diseases.

Acknowledgments

We thank Stephanie Elbin, Melanie Garbe, Roya Soltan, and Sara McCurdy for excellent technical assistance and Dr Mona Saffarzadeh for helpful discussions.

Sources of Funding

This work was supported in part by the Deutsche Forschungsgemeinschaft: FOR809, ZE-827/1-2, ZE-827/4-1 and SFB688 TPA12 to Dr Zernecke; PROMISE-IRTG-1566 and the Excellence Cluster Cardiopulmonary System to Dr Preissner; National Institutes of Health grants HL75677 and HL081863, and Hawaii Community Foundation grant 47037 to Dr Boisvert. Core facilities at the University of Hawaii were supported by P30GM103341. We are grateful for the support of a stipend (laboratory-rotation fellowship) from the "International Giessen-Graduate Center for the Life Sciences" (GGL) and by the Giessen-Kazan Partnership (Deutscher Akademischer Austauschdienst; DAAD; Bonn, Germany) to Cabrera-Fuentes.

Disclosures

None.

References

1. Weber C, Noels H. Atherosclerosis: current pathogenesis and therapeutic options. *Nat Med*. 2011;17:1410–1422.
2. Inoue T, Croce K, Morooka T, Sakuma M, Node K, Simon DI. Vascular inflammation and repair: implications for re-endothelialization, restenosis, and stent thrombosis. *JACC Cardiovasc Interv*. 2011;4:1057–1066.
3. Kannemeier C, Shibamiya A, Nakazawa F, Trusheim H, Ruppert C, Markart P, Song Y, Tzima E, Kennerknecht E, Niepmann M, von Bruehl ML, Sedding D, Massberg S, Günther A, Engelmann B, Preissner KT. Extracellular RNA constitutes a natural procoagulant cofactor in blood coagulation. *Proc Natl Acad Sci U S A*. 2007;104:6388–6393.
4. Fischer S, Preissner KT. Extracellular nucleic acids as novel alarm signals in the vascular system. Mediators of defence and disease. *Hamostaseologie*. 2013;33:37–42.
5. Fischer S, Gerriets T, Wessels C, Walberer M, Kostin S, Stolz E, Zheleva K, Hocke A, Hippenstiel S, Preissner KT. Extracellular RNA mediates endothelial-cell permeability via vascular endothelial growth factor. *Blood*. 2007;110:2457–2465.
6. Fischer S, Nishio M, Peters SC, Tschernatsch M, Walberer M, Weidemann S, Heidenreich R, Couraud PO, Weksler BB, Romero IA, Gerriets T, Preissner KT. Signaling mechanism of extracellular RNA in endothelial cells. *FASEB J*. 2009;23:2100–2109.

7. Fischer S, Grantzow T, Pagel JI, Tschernatsch M, Sperandio M, Preissner KT, Deindl E. Extracellular RNA promotes leukocyte recruitment in the vascular system by mobilising proinflammatory cytokines. *Thromb Haemost*. 2012;108:730–741.
8. Fischer S, Nishio M, Dadkhahi S, Gansler J, Saffarzadeh M, Shibamiyama A, Kral N, Baal N, Koyama T, Deindl E, Preissner KT. Expression and localisation of vascular ribonucleases in endothelial cells. *Thromb Haemost*. 2011;105:345–355.
9. Walberer M, Tschernatsch M, Fischer S, Ritschel N, Volk K, Friedrich C, Bachmann G, Mueller C, Kaps M, Nedelmann M, Blaes F, Preissner KT, Gerriets T. RNase therapy assessed by magnetic resonance imaging reduces cerebral edema and infarction size in acute stroke. *Curr Neurovasc Res*. 2009;6:12–19.
10. Han X, Kitamoto S, Wang H, Boisvert WA. Interleukin-10 overexpression in macrophages suppresses atherosclerosis in hyperlipidemic mice. *FASEB J*. 2010;24:2869–2880.
11. Shagdarsuren E, Bidzhekov K, Djalali-Talab Y, Liehn EA, Hristov M, Matthijsen RA, Buurman WA, Zernecke A, Weber C. C1-esterase inhibitor protects against neointima formation after arterial injury in atherosclerosis-prone mice. *Circulation*. 2008;117:70–78.
12. Shagdarsuren E, Djalali-Talab Y, Aurrand-Lions M, Bidzhekov K, Liehn EA, Imhof BA, Weber C, Zernecke A. Importance of junctional adhesion molecule-C for neointimal hyperplasia and monocyte recruitment in atherosclerosis-prone mice-brief report. *Arterioscler Thromb Vasc Biol*. 2009;29:1161–1163.
13. Cai W, Vosschulte R, Afsah-Hedjri A, Koltai S, Kocsis E, Scholz D, Kostin S, Schaper W, Schaper J. Altered balance between extracellular proteolysis and antiproteolysis is associated with adaptive coronary arteriogenesis. *J Mol Cell Cardiol*. 2000;32:997–1011.
14. Han X, Kitamoto S, Lian Q, Boisvert WA. Interleukin-10 facilitates both cholesterol uptake and efflux in macrophages. *J Biol Chem*. 2009;284:32950–32958.
15. Neu C, Sedlag A, Bayer C, Förster S, Crauwels P, Niess JH, van Zandbergen G, Frascaroli G, Riedel CU. CD14-dependent monocyte isolation enhances phagocytosis of listeria monocytogenes by proinflammatory, GM-CSF-derived macrophages. *PLoS One*. 2013;8:e66898.
16. Weber C, Aepfelbacher M, Haag H, Ziegler-Heitbrock HW, Weber PC. Tumor necrosis factor induces enhanced responses to platelet-activating factor and differentiation in human monocytic Mono Mac 6 cells. *Eur J Immunol*. 1993;23:852–859.
17. Tugal D, Liao X, Jain MK. Transcriptional control of macrophage polarization. *Arterioscler Thromb Vasc Biol*. 2013;33:1135–1144.
18. Rhee SH, Jones BW, Toshchakov V, Vogel SN, Fenton MJ. Toll-like receptors 2 and 4 activate STAT1 serine phosphorylation by distinct mechanisms in macrophages. *J Biol Chem*. 2003;278:22506–22512.
19. Wieczorek AJ, Rhyner C, Block LH. Isolation and characterization of an RNA-proteolipid complex associated with the malignant state in humans. *Proc Natl Acad Sci U S A*. 1985;82:3455–3459.
20. Ekström K, Valadi H, Sjöstrand M, Malmhäll C, Bossios A, Eldh M, Lötvall J. Characterization of mRNA and microRNA in human mast cell-derived exosomes and their transfer to other mast cells and blood cd34 progenitor cells. *J Extracell Vesicles*. 2012: 1–12.
21. Fischer S, Gesierich S, Griemert B, Schänzer A, Acker T, Augustin HG, Olsson AK, Preissner KT. Extracellular RNA liberates tumor necrosis factor-α to promote tumor cell trafficking and progression. *Cancer Res*. 2013;73:5080–5089.
22. Manka DR, Wiegman P, Din S, Sanders JM, Green SA, Gimple LW, Ragosta M, Powers ER, Ley K, Sarembock IJ. Arterial injury increases expression of inflammatory adhesion molecules in the carotid arteries of apolipoprotein-E-deficient mice. *J Vasc Res*. 1999;36:372–378.
23. Lucerna M, Zernecke A, de Nooijer R, de Jager SC, Bot I, van der Lans C, Kholova I, Liehn EA, van Berkel TJ, Yla-Herttuala S, Weber C, Biessen EA. Vascular endothelial growth factor-A induces plaque expansion in ApoE knock-out mice by promoting de novo leukocyte recruitment. *Blood*. 2007;109:122–129.
24. Schober A, Manka D, von Hundelshausen P, Huo Y, Hanrath P, Sarembock IJ, Ley K, Weber C. Deposition of platelet RANTES triggering monocyte recruitment requires P-selectin and is involved in neointima formation after arterial injury. *Circulation*. 2002;106:1523–1529.

CLINICAL PERSPECTIVE

Atherosclerosis remains the number one cause of death in the Western world, and the therapeutic options currently available are limited. Regarded as a chronic inflammatory disease of the vessel wall, monocytes/macrophages, inflamed smooth muscle cells, and several cytokines, proteases, and other molecular players, as well, contribute to disease development. Based on our previous studies concerning extracellular RNA (eRNA) as a novel alarm signal and potent cofactor in inflammation and thrombosis, we here investigated the contribution of the eRNA/RNase system during atherogenesis. In the experimental model of high-fat diet–induced atherosclerosis in low-density lipoprotein receptor–deficient and apolipoprotein E–deficient mice, eRNA accumulated in atherosclerotic plaques in a time-dependent manner, but was also released from activated cells, yielding increased plasma levels after arterial injury. In fact, eRNA functioned to promote inflammatory gene expression in macrophages and smooth muscle cells. Importantly, eRNA-degrading RNase1, administered via minipumps, significantly reduced plaque formation, monocyte recruitment, and vascular inflammation after injury. These data provide evidence for a major role of the eRNA/RNase system in atherogenesis and identify eRNA as an important trigger of inflammatory processes that fuel atherosclerotic lesion growth. These novel data extend our previous findings in which RNase1 was found to reduce infarction size in acute stroke. Thus, our study may harbor great potential for the establishment of RNase1 administration as a novel interventional strategy for the therapy of cardiovascular diseases. Because RNase1 is a thermostable, nontoxic enzyme, it bears several features that are applicable as a new interventional regimen against atherothrombotic disease.

SUPPLEMENTAL MATERIAL

Supplemental Methods

Arterial wire-induced injury

Wild-type and *Ldlr*$^{-/-}$ mice (both on the C57BL/6J background) were obtained from the Jackson Laboratory (Bar Harbor, ME, USA), and *apoE*$^{-/-}$ mice (C57BL/6J background) from Charles River, Italy. At 6 to 8 weeks of age mice were placed on an atherogenic diet (21% fat, 0,15% cholesterol, Altromin) for one week before and up to three weeks after injury. Animals were treated intravenously with a bolus of 0.76 µg RNase1 (in PBS) or PBS alone immediately before wire-induced injury and continuously treated with RNase1 via Alzet® osmotic minipumps (42 µg/kg mouse per day), subcutaneously implanted one day before injury. For induction of wire-induced injury, mice were anesthetised intraperitoneally with ketamine and xylazine. After midline neck incision, the left external carotid artery was tied off distally, and via transverse arteriotomy, a 0.014-in flexible angioplasty guidewire was advanced by 1 cm. Complete and uniform endothelial denudation was achieved by 3 passes along the common carotid artery with a rotating motion. All animal studies were approved by local authorities and complied with German animal protection law.

High-fat-diet driven atherosclerosis in LDL-receptor-deficient mice

C57BL/6J and *Ldlr*$^{-/-}$ *mice* (C57BL/6J background) were obtained from Jackson Laboratory and were fed with atherogenic diet as described[1].

Immunohistochemistry

For evaluation of neointima formation, mice were sacrificed at indicated time points, *in situ* fixed with 4 % paraformaldehyde, and carotid arteries were excised and embedded in paraffin. Neointimal and medial areas were quantified in serial sections (5 µm; 10 per mouse) within 500 µm from the bifurcation by Movat's pentachrome staining and planimetry of the areas within external elastic lamina, internal elastic lamina, or lumen (Diskus software, Hilgers). Adjacent sections were used to assess plaque cellular content by immunofluorescence staining of macrophages and SMCs by mAb staining for Mac2 (rat anti-mouse, Santa Cruz) and α-smooth muscle actin (mouse anti-human, Santa Cruz), respectively. Briefly, slides were blocked with 1% bovine serum albumin (Sigma Aldrich), incubated with primary antibody overnight at 4°C, and secondary detection performed using the relevant Alexafluor 488-conjugated antibody (Molecular Probes, Life Technologies, Germany). Sections were

counterstained with DAPI (1µg/mL; Merck, Darmstadt Germany) for visualisation of cell nuclei, then coverslipped using Vectorshield mounting medium (Vector Laboratories, Burlingame, USA). Images were recorded using a Leica DM-RXE fluorescence microscope, and quantified using Diskus software.

To determine the distribution of eRNA in atherosclerotic lesions, mice were sacrificed at indicated time points and perfused via the left ventricle with 10 ml PBS containing 1 mM EDTA and 30 ml fixative (PBS, 4% paraformaldehyde and 5% sucrose), and the atherosclerotic lesions were analyzed in the heart aortic valve as described previously[1]. Immunohistochemistry was performed on 5 µm cryostat tissue sections, fixed for 15 min in acetone at -20°C. SYTO® RNASelect™ dye (Invitrogen, USA) and the primary antibody recognizing rat anti-mouse MOMA-2 monoclonal antibody (Abcam, Cambridge, UK) against monocytes/macrophages were incubated for 1 h at room temperature followed by a secondary antibody conjugated with Cy3 (Abcam), or primary antibody against TNF-α (goat anti-mouse polyclonal, Santa Cruz) or Icam-1 (rat anti-mouse monoclonal, ebioscience), detected by FITC-konjugated secondary antibody (rabbit anti-goat IgG, goat anti-rat IgG, Jackson ImmunoResearch). Tissue sections were counterstained with DAPI (1µg/ml, Sigma Aldrich) for nuclei detection. Specimens were visualized using the confocal NIKON-microscope ECLIPSE TE200-E (Nikon, Düsseldorf, Germany), sections were taken through the tissue at 0.25 µm intervals, and analyzed by image acquisition software EZ-C1 Goldversion 3.8.

Confocal microscopy and quantification of RNA

Cryosections (5 µm thick) of aortic sinus from *Ldlr*$^{-/-}$ mice were air dried and fixed with 4% paraformaldehyde and then incubated with 1% bovine serum albumin for 30 min to block non-specific binding sites. After rinsing in PBS, the samples were incubated 2 h at room temperature with primary antibodies against smooth muscle α-actin TRITC-labeled (Sigma). After repeated washes with PBS, the tissue sections were incubated with SYTO® RNASelect™ dye (Invitrogen) used for RNA localization. Nuclei were visualized with DAPI (Molecular Probes). Tissue sections were examined by laser scanning confocal microscopy (Leica TCS SP2), and confocal optical sections were taken using a Leica x63/1.32 objective lens. Each recorded image was taken using multi-channel scanning and consisted of 1024 x 1024 pixels. To improve image quality and to obtain a high signal to noise ratio, each image from the series was signal-averaged and was deconvoluted using AutoQuant X2 software (Bitplane, Zürich, Switzerland). For three-dimensional image reconstructions, an Imaris 6.3.1 multichannel image processing software (Bitplane) was used.

For quantification of the eRNA, all tissue samples were simultaneously immunolabeled under identical conditions of fixation and dilutions of primary and secondary antibodies. Ten randomly chosen fields of vision were quantified using three-dimensional "Quantification" and "VoxelShop" options of Imaris 6.3.1 (Bitplane). The area of specific labeling for eRNA was calculated as arbitrary fluorescent units of positive labelling, each for the media area or neointima area, as previously described.[2]

Intravital imaging

For intravital microscopy, 0.05% rhodamine-G (Molecular Probes) was administered *i.v.* to *apoE*$^{-/-}$ mice fed an atherogenic diet and treated with RNase or vehicle (PBS) 1 day after injury. Carotid arteries were exposed in anesthetized mice (100 mg/kg bodyweight ketamine and 10 mg/kg bodyweight xylazine). Arrest of labeled leukocytes was visualized by epifluorescence microscopy (Olympus BX51, 20x water immersion), and recorded using a digital camera (Hamamatsu EM-CCD, C9100) and analysed using Cell-R software (Olympus).

Isolation of extracellular RNA and real time PCR analysis

DNA-free total RNA was extracted from plasma of mice ~~or~~, from supernatants of SMC or SMC using Zymo RNA MicroPrep kit (Zymo Research) omitting a lysis step and with an additional DNase digestion step. Total RNA (10 ng) was reverse-transcribed at 37°C for 1 h. cDNA fragments were amplified by 45 cycles of PCR (denaturing at 95°C for 15 s, annealing at 58°C for 30 s, and extension at 72°C for 30 s); the last extension was performed at 50°C for 2 min. The following primers were used:

Mouse *Cd31* forward 5'-CTCCAACAGAGCCAGCAGTA-3',
mouse *Cd31* reverse 5'-GACCACTCCAATGACAACCA-3',
mouse *Sma* forward 5'-CTGACAGAGGCACCATGAA-3',
mouse *Sma* reverse 5'-AGAGGCATAGAGGGACAGCA-3',
mouse *Gapdh* forward 5'-CACTCAAGATTGTCAGC-3',
mouse *Gapdh* reverse 5'-CCACAGCCTTGGCAGC-3'.
mouse *Icam-1* forward 5'-GCCTTGGTAGAGGTGACTGAG-3'
mouse *Icam-1* reverse 5'-GACCGGAGCTGAAAAGTTGTA-3'
mouse *Vcam-1* forward 5'-TGCCGAGCTAAATTACACATTG-3'
mouse *Vcam-1* reverse 5'-CCTTGTGGAGGGATGTACAGA-3'
mouse *P-selectin* forward 5'-AGGGAAATGATGCCATTCAG-3'
mouse *P-selectin* reverse 5'-ACCGGAAACTCTGGACATTG-3'

mouse *Ccl2* forward 5'-GATGCAGTTAACGCCCCACT-3'
mouse *Ccl2* reverse 5'-AGCTTCTTTGGGACACCTGC-3'
mouse *Tnf-α* forward 5'-ACTGAACTTCGGGGTGATCG-3'
mouse *Tnf-α* reverse 5'-GGCTACAGGCTTGTCACTCG-3'
mouse *Il-1β* forward 5'-GGATGAGGACATGAGCACCT-3'
mouse *Il-1β* reverse 5'-GGAGCCTGTAGTGCAGTTGT-3'
mouse *Il-6* forward 5'-ATGGATGCTACCAAACTGGAT-3'
mouse *Il-6* reverse 5'-TGAAGGACTCTGGCTTTGTCT-3'

After incubation with or without eRNA (1 - 25 μg/ml), total cellular RNA was extracted from BMDM using TRIzol® Reagent (Invitrogen, USA). RNA samples were then subjected to RNA purification using the RNeasy minikit (Qiagen, USA). One μg of DNase-treated total RNA was reverse-transcribed using GoScript™ Reverse Transcription System (Promega, USA). Real-time quantitative RT-PCR (q-PCR) was performed at Genomics Core Facility, John A. Burns School of Medicine, Hawaii. The gene products were quantified using SYBR Green assays (Applied Biosystems). mRNA signal from GAPDH was used for normalization. The 50 pmol of each primer was used with the following sequences:
Mouse *Gapdh* forward 5'-GGCAAATTCAACGGCACAG-3',
mouse *Gapdh* reverse 5'-CGCTCCTGGAAGATGGTGA-3',
mouse *Il-1β* forward 5'-GGGCCTCAAGGAAAAGAATC-3',
mouse *Il-1β* reverse 5'-TTCTCCTTGAGAGGTGCTCA-3',
mouse *Tnf-α* forward 5'-CATCTTCTCAAAATTCGAGTGACAA-3',
mouse *Tnf-α* reverse 5'-TGGGAGTAGACAAGGTACAACCC-3',
mouse *Il-6* forward 5'-GAGGATACCACTCCCAACAGACC-3',
mouse *Il-6* reverse 5'-AAGTGCATCATCGTTGTTCATACA-3',
mouse *Inf-γ* forward 5'-TGGCTCTGCAGGATTTTCAT-3',
mouse *Inf-γ* reverse 5'-TCAAGTGGCATAGATGTGGA-3',
mouse *Il-10* forward 5'-TGCACTACCAAAGCCACAAGG-3',
mouse *Il-10* reverse 5'-TGGGAAGTGGGTGCAGTTATTG-3',
mouse *Il-4* forward 5'-CAACGAAGAACACCACAGAGAG-3',
mouse *Il-4* reverse 5'-ATGAATCCAGGCATCGAAAAGC-3',
mouse *Arg2* forward 5'-CCTCCCTGCCAATCATGTTC-3',
mouse *Arg2* reverse 5'-CCTCCCTGCCAATCATGTTC-3',
mouse *Il-12* forward 5'-CCCTGTGCCTTGGTAGCATC-3',

mouse *Il-12* reverse 3'-CTGAAGTGCTGCGTTGATGG-3',
mouse *iNOS* forward 5'-CTCTGGTCTTGCAAGCTGATGGTCA-3',
mouse *iNOS* reverse 5'- TCCTGGAACCACTCGTACTTGGGAT-3',

Cell culture and cell adhesion assay under flow

Human coronary artery SMC (Promocell) and MonoMac6 cells were maintained as described[3, 4]. MonoMac6 cell adhesion to SMC was analyzed in parallel wall flow-chambers[3]. Confluent SMC were activated with TNF-α (50 ng/ml) in the absence or presence of RNase1 (10 µg/ml) for 16 h. Likewise, MonoMac6 cells were left untreated or pretreated with RNase1 (10 µg/ml) for 16 h and suspended (at $1x10^6$ cells/ml) in HH-medium (1x Hank's buffered saline solution, containing 10 µM HEPES and 5 mg/ml bovine serum albumin). Confluent SMC were activated with TNF-α (50 ng/ml) followed by treatment with buffer alone or RNase1 (10 µg/ml) for 16 h. Prior to the experiment, $CaCl_2$ and $MgCl_2$ (each at 1 mM) were added to MonoMac6 cells, which were perfused over SMC at 1.5 dyne/cm^2. After 5 min, firm adherence of cells was assessed by phase-contrast video microscopy and quantified in multiple fields recorded with a JVC 3CCD video camera.

Viability assay

After treating SMC or MM6 with RNase1 (10 µg/ml) for 30 min or 16 h, respectively, viability assays were performed by using the fluorescent CellTiter-Blue® cell viability assay (Promega) according to the manufacturer's instructions.

Statistics

Data were analyzed by unpaired Student t tests, and if more than 2 groups were compared by ANOVA 1-way analysis of variance followed by Tukey's or Dunnett's multiple comparison post tests. Differences with $p<0.05$ were considered to be statistically significant. Analyses for Figures 5A-C, and Figure 7B were performed using two tailed t-tests. Analyses for Figure 2L and 4A were performed using a one-way ANOVA followed by Tukey multiple comparison test. Analysis for Figure 2A, 3A-D, 4B-C, 6A-G, 7B and Supplemental Figure 1 and 3 were performed using a one-way ANOVA followed by Dunnett's multiple comparison test. Statistical analyses were performed using Graph Pad Prism 6.0.

Supplemental Figures

Supplemental Figure 1

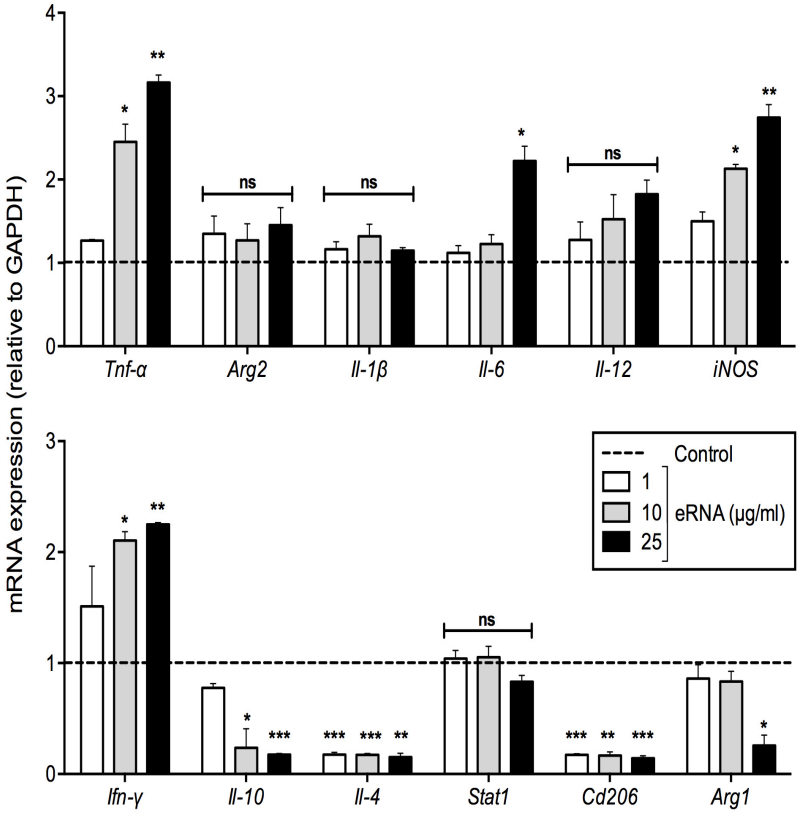

Supplemental Figure 1. mRNA expression of *Tnf-α, Arg2, Il-1β, Il-6*, *Il-12, iNOS, Ifn-γ, Il-10*, *Il-4*, *Stat1, Cd206* and *Arg1* in wild-type BMDM, differentiated in the presence of mouse recombinant GM-CSF was analyzed by real-time PCR in the absence (control, dotted line) or presence of eRNA (1, 10, or 25 µg/ml) for 24 h. Data are expressed as changes in the ratio between target gene expression and *Gapdh* mRNA. Values represent mean ± SD (n=6 per group); *p<0.05, **p<0.01, ***p<0.001 *vs*. control, ns = non-significant.

Supplemental Figure 2

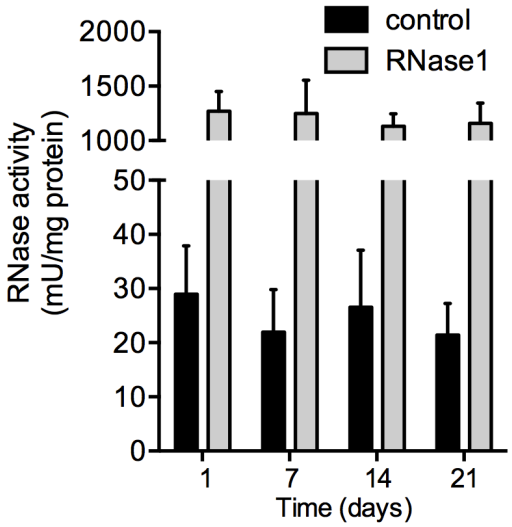

Supplemental Figure 2. RNase activity in plasma of *apoE*$^{-/-}$ mice at indicated time points after arterial injury in the control and the RNase1 treatment group (n=4 per group). Values represent mean ± SEM.

Supplemental Figure 3

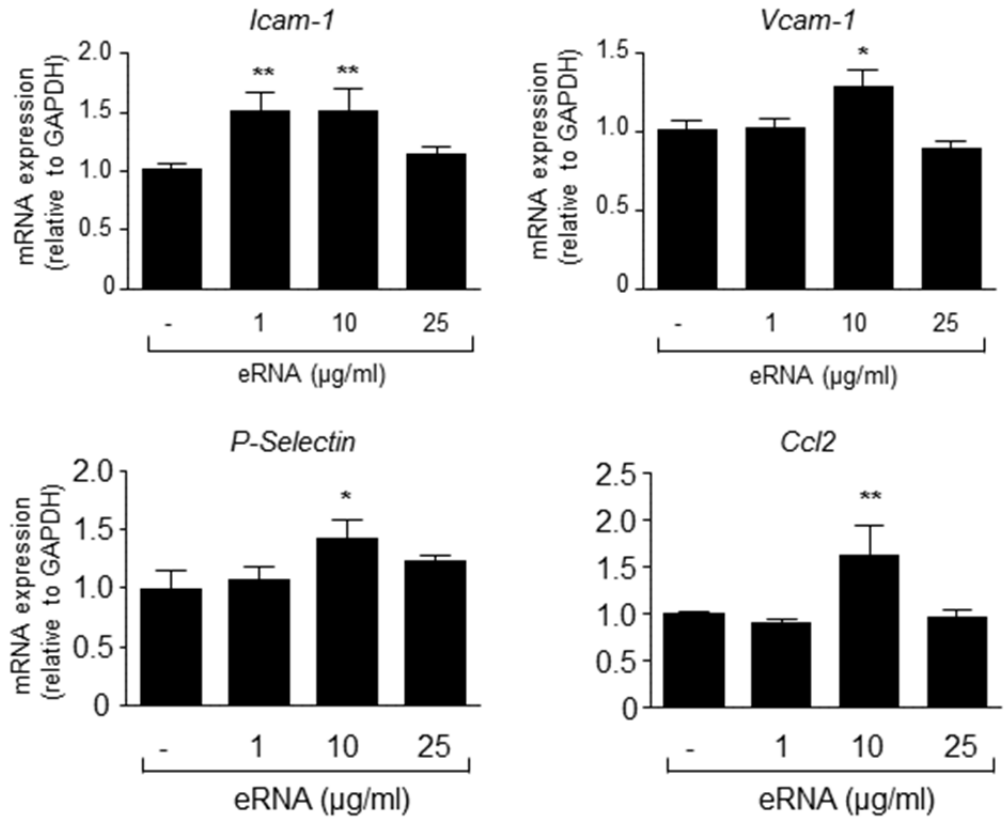

Supplemental Figure 3. mRNA expression of *Icam1, Vcam1, P-selectin* and *Ccl2* in SMC was analyzed by real-time PCR in the absence or presence of eRNA (1, 10, or 25 µg/ml) after 16 hours (n=9 per group). Values represent mean ± SEM; *p<0.05, **p<0.01 vs. unstimulated controls.

Supplemental References

1. Han X, Kitamoto S, Wang H, Boisvert WA. Interleukin-10 overexpression in macrophages suppresses atherosclerosis in hyperlipidemic mice. *FASEB*. 2010;24:2869-2880
2. Cai W, Vosschulte R, Afsah-Hedjri A, Koltai S, Kocsis E, Scholz D, Kostin S, Schaper W, Schaper J. Altered balance between extracellular proteolysis and antiproteolysis is associated with adaptive coronary arteriogenesis. *J Mol Cell Cardiol*. 2000;32:997-1011
3. Shagdarsuren E, Bidzhekov K, Djalali-Talab Y, Liehn EA, Hristov M, Matthijsen RA, Buurman WA, Zernecke A, Weber C. C1-esterase inhibitor protects against neointima formation after arterial injury in atherosclerosis-prone mice. *Circulation*. 2008;117:70-78
4. Weber C, Aepfelbacher M, Haag H, Ziegler-Heitbrock HW, Weber PC. Tumor necrosis factor induces enhanced responses to platelet-activating factor and differentiation in human monocytic mono mac 6 cells. *Eur J Immunol.* 1993;23:852-859